DEMOGRAPHIC RESEARCH
A peer-reviewed, open-access journal of population sciences

DEMOGRAPHIC RESEARCH

VOLUME 48, ARTICLE 27, PAGES 809–828
PUBLISHED 17 MAY 2023
http://www.demographic-research.org/Volumes/Vol48/27/
DOI: 10.4054/DemRes.2023.48.27

Formal Relationship

Improved bounds and high-accuracy estimates for remaining life expectancy via quadrature rule-based methods

Oscar E. Fernandez

© 2023 Oscar E. Fernandez.

This open-access work is published under the terms of the Creative Commons Attribution 3.0 Germany (CC BY 3.0 DE), which permits use, reproduction, and distribution in any medium, provided the original author(s) and source are given credit.
See https://creativecommons.org/licenses/by/3.0/de/legalcode

Contents

Improved bounds and high-accuracy estimates for remaining life expectancy via quadrature rule-based methods

Oscar E. Fernandez[1]

Abstract

BACKGROUND
Previous research has derived bounds on the remaining life expectancy function $e(x)$ that connect survivorship and remaining life expectancy at two age values and therefore can be used to, among other things, estimate life expectancy at birth when the population's full mortality trajectory is not known.

RESULTS
We show that the aforementioned bounds emerge from using particular two-node closed quadrature rules and prove a theorem that establishes conditions for when an n-node closed rule respects those bounds for $e(x)$. This enables the usage of known high-accuracy rules that stay within the bounds and provide new high-accuracy estimates for $e(x)$. We show that among this set of rules are ones that yield exact estimates for $e(x)$. We illustrate our work empirically using life table data from French females since 1816 and discover a new empirical regularity linking life expectancy at birth in the data set to survivorship and remaining life expectancy at age 20.

CONTRIBUTION
Our results furnish conditions for using known rules to generate high-accuracy estimates of remaining life expectancy that respect the known theoretical bounds on $e(x)$, making calculating the associated maximum errors straightforward and requiring no information about the higher-order derivatives of the associated survival function, as is the case for standard rules. The empirical validation of this approach in the French female data and the discovery of the aforementioned associated empirical regularity argue for follow-up research using our approach to establish additional, higher-accuracy estimates for $e(x)$ and also to probe the generality and biodemographic drivers of the new regularity.

[1] Department of Mathematics, Wellesley College, Wellesley, MA 02482. Email: ofernand@wellesley.edu.

1. Background

Consider an age-structured population in which the maximum life span is ω. Let $s(x)$ denote the associated survival function, where age x is measured in years, and $e(x)$ denote the remaining life expectancy at age x. By definition, $s(x)$ is a nonincreasing function, and $s(0) = 1$, $s(\omega) = e(\omega) = 0$, and $e(0) = e_0$, the life expectancy at birth. Assuming $s(x)$ is a continuous function, Cohen (2011) proves that

$$(b - a + e(b))\frac{s(b)}{s(a)} \leq e(a) \leq b - a + e(b)\frac{s(b)}{s(a)}, \qquad 0 \leq a \leq b \leq \omega. \tag{1}$$

When $a = b$ this equation reduces to the unenlightening $e(a) \leq e(a) \leq e(a)$. We will therefore discuss here only the $a < b$ case. Furthermore, when $s(x)$ is nonconstant on $[a, b]$–a realistic assumption for real-world populations–the inequalities in Equation 1 become strict. These assumptions transform Equation 1 into

$$(b - a + e(b))\frac{s(b)}{s(a)} < e(a) < b - a + e(b)\frac{s(b)}{s(a)}, \qquad 0 \leq a < b \leq \omega. \tag{2}$$

As Cohen (2011) discusses, the bounds here can be used to approximate $e(x)$ (e.g., $e(0) = e_0$) using $e(y)$ and $s(y)$, where $y \neq x$, making possible the estimation of life expectancy without detailed knowledge of the mortality trajectory between ages x and y.

In this article we derive Equation 2 using a different method than the one used by Cohen (2011). Herein, we take a numerical analysis approach. In Section 2 we first show that Equation 2 is built from a 0-degree accurate two-node closed quadrature rule (the Appendix reviews these concepts) and then provide conditions under which such quadrature rules respect the bounds in Equation 2. We then use this to develop higher accuracy quadrature rule approximations to $e(x)$. In particular, we show that among these quadrature rules is one that evaluates $e(x)$ exactly. Section 3 explores the accuracy of the new approximations developed: we profile one such approximation that halves the maximum error incurred by using either of the bounds in Equation 2 and show how those accuracies may be improved. We investigate our results empirically in Section 4 using life table data from French females since 1816 and present a new empirical regularity linking life expectancy at birth in the data set to survivorship and remaining life expectancy at age 20. In the Discussion section we comment on this new regularity and discuss potential follow-up investigations.

2. Results and new relationships

Theorem 1. Let a and b be such that $0 \leq a < b \leq \omega$. Suppose that $s(x)$ is continuous, nonincreasing, and nonconstant on $[a, b]$, with $s(a) \neq 0$. Then

$$(b-a)s(b) < \int_a^b s(t)\,dt < (b-a)s(a), \tag{3}$$

and from this follows Equation 2.

Proof. The assumptions on s imply that $s(b) < s(t) < s(a)$ for $t \in [a, b]$. Integrating this inequality yields Equation 3. To show how Equation 3 yields Equation 2, we note that since

$$\begin{aligned} \int_a^b s(t)\,dt &= \int_a^b s(t)\,dt + \int_b^\omega s(t)\,dt - \int_b^\omega s(t)\,dt \\ &= \int_a^\omega s(t)\,dt - \int_b^\omega s(t)\,dt \\ &= e(a)s(a) - e(b)s(b), \end{aligned} \tag{4}$$

substituting this into Equation 3 yields $(b-a)s(b) < e(a)s(a) - e(b)s(b) < (b-a)s(a)$. Solving this for $e(a)$ and using the assumption that $s(a) \neq 0$ yields Equation 2. □

The bounds in Equation 3–for easy reference, hereafter we refer to those as the 'Cohen bounds'–are what result from using a 0-degree accurate two-node closed quadrature rule for s on $[a, b]$ (c.f., the Appendix). This theorem, therefore, shows that this type of quadrature rule undergirds Equation 2. Using a higher-degree accurate quadrature rule would generate a more accurate $e(a)$ estimate. But the error expressions for quadrature rules generally involve the higher-order derivatives of the integrand (Burden, Faires, and Burden 2015), in this case $s(t)$. Without knowledge of those higher-order derivatives one cannot *a priori* know (or even bound) the error incurred in a general quadrature rule. This is one strength of Equation 2: The maximum error (the difference in the bounds) is explicitly calculable from life tables. The next theorem furnishes conditions under which a two-node closed quadrature rule respects the Cohen bounds.

Theorem 2. Let a and b be such that $0 \leq a < b \leq \omega$. Suppose that $s(x)$ is continuous, nonincreasing, and nonconstant on $[a, b]$, with $s(a) \neq 0$. For the two-node closed

quadrature rule $\int_a^b s(t)\,dt \approx c_1 s(a) + c_2 s(b)$, if

$$c_1 \geq 0, \qquad c_2 \geq 0, \qquad c_1 + c_2 = b - a, \tag{5}$$

then

$$(b-a)s(b) < \int_a^b s(t)\,dt \approx c_1 s(a) + c_2 s(b) < (b-a)s(a) \tag{6}$$

and

$$[(b-a) + e(b)]\frac{s(b)}{s(a)} < e(a) \approx \frac{c_1 s(a) + [c_2 + e(b)]s(b)}{s(a)} < (b-a) + e(b)\frac{s(b)}{s(a)}. \tag{7}$$

Proof. The nonconstant and nonincreasing properties of $s(x)$ on $[a, b]$ imply that $s(a) > s(b)$. Using now the assumptions in Equation 5 we get

$c_1 s(a) + c_2 s(b) < c_1 s(a) + c_2 s(a) = (c_1 + c_2)s(a) = (b-a)s(a)$ and
$c_1 s(a) + c_2 s(b) > c_1 s(b) + c_2 s(b) = (c_1 + c_2)s(b) = (b-a)s(b)$.

Thus, using Equation 3 we get bounds for the two-node closed quadrature rule that proves Equation 6:

$$(b-a)s(b) < c_1 s(a) + c_2 s(b) \approx \int_a^b s(t)\,dt \text{ and } \int_a^b s(t)\,dt \approx c_1 s(a) + c_2 s(b) < (b-a)s(a).$$

To prove Equation 7, substitute Equation 4 into Equation 6 to get

$$(b-a)s(b) < e(a)s(a) - e(b)s(b) \approx c_1 s(a) + c_2 s(b) < (b-a)s(a).$$

Solving this for $e(a)$ and making use of the assumption that $s(a) \neq 0$ yields Equation 7. □

Corollary 1. Let a and b be such that $0 \leq a < b \leq \omega$. Suppose that $s(x)$ is continuous, nonincreasing, and nonconstant on $[a, b]$, with $s(a) \neq 0$. Then for every $t \in (0, 1)$,

$$[(b-a) + e(b)]\frac{s(b)}{s(a)} < e(a) \approx \frac{(b-a)[s(a) + t(s(b) - s(a))] + e(b)s(b)}{s(a)} < (b-a) + e(b)\frac{s(b)}{s(a)}. \tag{8}$$

Furthermore, there exists $\xi \in (0,1)$ such that

$$e(a) = \frac{(b-a)[s(a) + \xi_{a,b}(s(b) - s(a))] + e(b)s(b)}{s(a)}. \tag{9}$$

Proof. Let $t \in (0,1)$, $c_1 = (1-t)(b-a)$, and $c_2 = t(b-a)$. Then Equation 5 is satisfied for this combination of c-values and for each $t \in (0,1)$, and substituting these c-values into Equation 7 yields Equation 8.

To prove the last part we first note that the choice of c-values above converts the two-node closed quadrature rule $\int_a^b s(t)\,dt \approx c_1 s(a) + c_2 s(b)$ into

$$\int_a^b s(t)\,dt \approx \{s(a) + t[s(b) - s(a)]\}\,(b-a). \tag{10}$$

If $s(x)$ is continuous on $[a,b]$, then by the mean value theorem for integrals there exists a $t^* \in [a,b]$ such that

$$\int_a^b s(t)\,dt = s(t^*)\int_a^b 1\,dt = s(t^*)(b-a). \tag{11}$$

But because we have assumed that $s(x)$ is nonconstant on $[a,b]$ we cannot have $t^* = a$ or $t^* = b$. (When $t^* = a$ or $t^* = b$, Equation 11 violates the inequality of Equation 3.) Thus, $t^* \in (a,b)$. Substituting Equation 10 and Equation 11 into Equation 6 and then dividing by $b-a$ yields

$$s(b) < s(t^*) \approx s(a) + t[s(b) - s(a)] < s(a). \tag{12}$$

Define now the function $f(t)$ by $s(a) + t[s(b) - s(a)]$. This is a continuous (linear) function on $[0,1]$ with negative slope since $s(a) > s(b)$, and therefore by the intermediate value theorem it takes on every value between $f(0) = s(a)$ and $f(1) = s(b)$. Since $s(b) < s(t^*) < s(a)$ from Equation 12, there is therefore a $\xi_{a,b} \in (0,1)$ such that $f(\xi_{a,b}) = s(t^*)$. For that ξ-value,

$$\int_a^b s(t)\,dt = \{s(a) + \xi_{a,b}[s(b) - s(a)]\}\,(b-a). \tag{13}$$

Substituting this into the left-hand side of Equation 4 and solving for $e(a)$ then yields Equation 9. □

Corollary 1 provides a continuous family of two-node closed quadrature rules respecting the Cohen bounds. For the particular case of $t = 1/2$, Equation 8 yields

$$[(b-a)+e(b)]\frac{s(b)}{s(a)} < e(a) \approx \frac{(b-a)[s(a)+s(b)]}{2s(a)} + e(b)\frac{s(b)}{s(a)} < (b-a)+e(b)\frac{s(b)}{s(a)}. \quad (14)$$

Since the approximation herein is the same as that obtained from approximating $\int_a^b s(t)\,dt$ via the trapezoidal rule (because the right-hand side of Equation 10 reduces to the trapezoidal approximation when $t = 1/2$), we will refer to the approximation in Equation 14 as the trapezoidal estimate of $e(a)$. We note that if $s(x)$ is concave (or, respectively, convex) on $[a, b]$, then the trapezoidal estimate of $e(a)$ is a lower (or, respectively, upper) bound for $e(a)$ that is strictly greater (or, respectively, less) than the lower (or, respectively, upper) bound in Equation 2. These results are intuitively clear from Figure 1. The following theorem shows that this trapezoidal estimate halves the maximum error in estimating $e(a)$ as compared to using either of the Cohen bounds.

Figure 1: **Plots of $s(x)$ (blue curves) along with the line segments defined by $y = s(a)$ (black, dashed), $y = s(b)$ (red, dashed), and the line connecting $(a, s(a))$ and $(b, s(b))$ (gray, dashed)**

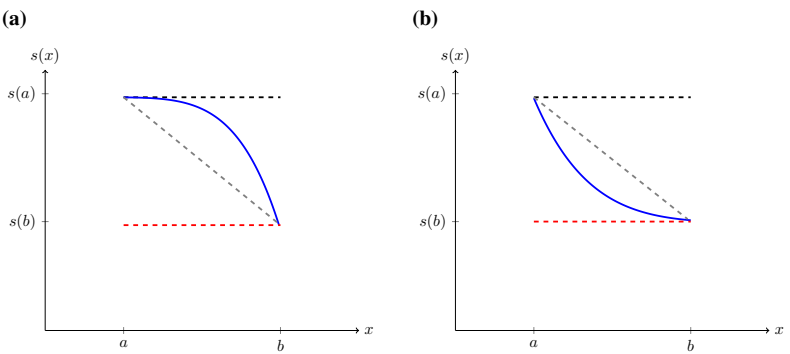

Note: The quantity $\int_a^b s(t)\,dt$ is better approximated by $(b-a)s(a)$ than by $(b-a)s(b)$ when $s(x)$ is concave on $[a, b]$ (a), and better approximated by $(b-a)s(b)$ than by $(b-a)s(a)$ when $s(x)$ is convex on $[a, b]$ (b).

Theorem 3. Let a and b be such that $0 \le a < b \le \omega$. Suppose that $s(x)$ is continuous, nonincreasing, and nonconstant on $[a, b]$, with $s(a) \neq 0$. Then the maximum error in

estimating $e(a)$ by Equation 14 is half the maximum error in estimating $e(a)$ by either bound in Equation 2.

Proof. Let U and L denote the upper and lower bounds in Equation 2. The maximum error incurred in using either of the bounds in Equation 2 to approximate $e(a)$–which we will denote by ME–is then

$$\begin{aligned} ME &= U - L \\ &= \left[(b-a) + e(b)\frac{s(b)}{s(a)}\right] - \left[(b-a+e(b))\frac{s(b)}{s(a)}\right] \\ &= (b-a)\left(1 - \frac{s(b)}{s(a)}\right). \end{aligned} \tag{15}$$

Denoting now the trapezoidal estimate in Equation 14 by T, Equation 14 says that $L < e(a) \approx T < U$. Thus, $e(a)$ must be contained in the interval $(L, T]$ or $[T, U)$. Since $T - L$ and $U - T$ are given by

$$\left[\frac{(b-a)[s(a)+s(b)]}{2s(a)} + e(b)\frac{s(b)}{s(a)}\right] - L = \frac{b-a}{2}\left(1 - \frac{s(b)}{s(a)}\right) = \frac{ME}{2}, \tag{16}$$

$$U - \left[\frac{(b-a)[s(a)+s(b)]}{2s(a)} + e(b)\frac{s(b)}{s(a)}\right] = \frac{b-a}{2}\left(1 - \frac{s(b)}{s(a)}\right) = \frac{ME}{2}, \tag{17}$$

respectively, we conclude that the estimate $e(a) \approx T$ halves the maximum error Equation 15. □

3. Applications and extensions of the theoretical results

3.1 Applications of the trapezoidal estimate

The improved accuracy of the trapezoidal estimate of $e(a)$ to the Cohen bounds makes possible more accurate estimates of, for example, life expectancy at birth. To wit, setting $a = 0$ in Equation 14 yields

$$e_0 \approx \frac{b}{2}[1 + s(b)] + e(b)s(b), \qquad 0 < b \leq \omega, \tag{18}$$

and Equation 17 assures us that this approximation halves the maximum error incurred relative to using either of the bounds in Equation 2. (We will refer to Equation 18 as the trapezoidal estimate of e_0.) As a concrete illustration of this let us set b equal to the median age m (for which $s(m) = 1/2$) in Equation 18; this yields

$$\frac{m + e(m)}{2} < e_0 \approx \frac{1.5m + e(m)}{2} < \frac{2m + e(m)}{2}, \tag{19}$$

where we have included the bounds that result from Equation 2 for comparison. The maximum error in using either of the bounds in Equation 19 to estimate e_0 is $ME = m/2$, whereas the maximum error in using the trapezoidal estimate is $ME = m/4$.

3.2 Additional high-accuracy approximation options

Incorporating additional knowledge about $s(x)$ or using more advanced quadrature rules or both improves the approximations to $e(a)$. As an example of the former, let us return to the notes in Figure 1 regarding how the convexity of the survival curve affects the estimate we have developed. In modern industrialized societies $s(x)$ is mostly convex for $x \lessapprox 2$ years and then becomes mostly concave until $x \approx 90$ years. These are therefore contexts in which, for example, using t-values close to 1 in the approximation in Equation 8 would yield accurate estimates of e_0 if we take $b = 20$, whereas using t-values close to 0 would yield accurate approximations of e_0 if we take $b = 80$. We illustrate this empirically in the next section.

Although we have restricted attention to two-node closed quadrature rules, Theorem 2 easily generalizes to handle n-node quadrature rules. To wit, if we replace the two-node quadrature rule in the theorem with an n-node one,

$$\int_a^b s(t)\,dt \approx \sum_{i=1}^{n} c_i s(x_i), \qquad \text{where we fix } x_1 = a \text{ and } x_n = b \tag{20}$$

and where n is a natural number, with $n \geq 3$, then under the hypotheses

$$c_i \geq 0, \qquad \sum_{i=1}^{n} c_i = b - a \tag{21}$$

(the analogues of Equation 5 in this n-node case), the same techniques used in the proof of Theorem 2 yield the n-node analogues of Equations 6 and 7, which are simply the

corresponding approximations where $c_1 s(a) + c_2 s(b)$ is replaced by the right-hand side in Equation 20. One can then employ more advanced quadrature methods to further improve the accuracy of the new quadratures in Equation 20. In particular, the Gauss-Lobatto quadrature rules satisfy the hypotheses in Equation 21 (Stoer and Burlisch 1993) and are known to exhibit high accuracy: The n-node Gauss-Lobatto rule has degree of accuracy $2n - 1$ (Stoer and Burlisch 1993). Given that polynomials of order as low as 8 yield fairly accurate fits to survival curves, $n = 4$ Gauss-Lobatto quadrature rules should generate high-accuracy approximations to $e(a)$. (For $n \geq 4$ these rules require $s(x)$- and $e(x)$-values at irrational x-values, but these can be estimated by interpolating between nearby integer x-values.)

Some existing parametric models for $s(x)$ can also be utilized within our framework. Specifically, any parametric model that satisfies $s(b) \leq s(x) \leq s(a)$ for $x \in [a, b]$ will generate an approximation for $e(a)$ that respects the bounds in Equation 2. (The quantity $c_1 s(a) + c_2 s(b)$ in Equation 6 is replaced by the output of $\int_a^b s(t)\, dt$ for the chosen parametric model, and thus Equation 7 follows from the same manipulations as in the proof of that part of Theorem 2.) For example, the functions

$$h_n(x) = s(a) - \left[\frac{s(a) - s(b)}{(b-a)^n}\right](x-a)^n, \qquad n > 0, \tag{22}$$

satisfy $s(b) \leq s(x) \leq s(a)$ for $x \in [a, b]$. These functions are convex for $0 < n < 1$ and concave for $n > 1$ ($h_1(x)$ is a linear function). Thus, if one has information about the concavity/convexity of $s(x)$ on $[a, b]$, then one can select appropriate n-values to generate accurate estimates of $e(a)$. As another example one could choose to model $s(x)$ as Weon and Je (2012) do, where a rescaled age $\frac{x}{\alpha}$ is used: $s\left(\frac{x}{\alpha}\right) = e^{-(x/\alpha)^{\beta(x/\alpha)}}$ (here $s(\alpha) = e^{-1}$ and $\beta(x)$ is a positively sloped linear function), suitably scaled to satisfy $s(b) \leq s(x) \leq s(a)$ for $x \in [a, b]$. Such modified stretched exponential survival models have been shown to accurately capture the post-1950 scale and shape variances in survival curves in human populations (Weon and Je 2012) and could therefore provide additional high-accuracy estimates of $e(a)$.

4. Applications to the remaining life expectancy in French females, 1816–2015

We now illustrate the theoretical results from Section 2 empirically using life table data from the Human Mortality Database HMD for French females (1816–2015, 200 yearly life tables).

Figures 2–6 plot the magnitude of the percentage errors in estimating e_0 for each

life table in the data set by the Cohen bounds and by the trapezoidal estimate in Equation 14 for $a = 0$ and $b = 20$, 40, 60, and 80. Accuracy generally increases over time for each of the three estimates, regardless of the b-value used. Figure 6 explains why: The rectangularization of the survival curves over time leads to $s(x)$ curves that are more nearly constant for $0 \leq x \leq b$, which leads to smaller $s(b) - s(0)$ values, which in turn shrinks the maximum errors defined by Equations 15, 16, and 17. The $b = 20$ estimates are, broadly speaking, the most accurate of the four (compare the range of the vertical axes in the figures). The reason here is simple: As the b-value increases there is more survival curve area that is underestimated by the lower Cohen bound and overestimated by the upper Cohen bound. As the b-value increases the lower Cohen bound becomes less accurate than the upper Cohen bound earlier in the data set. The reason for this goes back to our earlier observation about how the convexity of s affects these estimates (c.f., the Figure 1 caption). As Figure 6 shows, for $0 \leq x \leq 20$ the population's survival curves remain more convex than concave. This implies that the lower Cohen bounds are more accurate estimates than the upper ones. However, on the interval $0 \leq x \leq 80$ Figure 6 shows that the population's survival curves become more concave than convex over time. This implies that over time the upper Cohen bound estimates become more accurate than the lower bound estimates. These accuracy–concavity relationships also explain the dependency of the most accurate estimate on the b-value and time. For example, for $b = 40$ and 60 the trapezoidal estimate is generally the most accurate of the three (Figures 3 and 4). This accords with the fact that survival curves are roughly half-concave and half-convex over the intervals $0 \leq x \leq 40$ and $0 \leq x \leq 60$ (Figure 6). By contrast, for $b = 20$ the lower (Cohen) bound is generally the most accurate (Figure 2). (The trapezoidal estimate is just as accurate post-1975.) This accords with the enduring overall convexity of the survival curves over the interval $0 \leq x \leq 20$ (Figure 6). Finally, when $b = 80$ the upper Cohen bound is the most accurate post-1950 (Figure 5). This accords with the increasing degree of concavity of the survival curves over the interval $0 \leq x \leq 80$ post-1950 (Figure 6).

Figure 2: **Comparisons of the percentage error in using the lower bounds (red), upper bounds (blue), and trapezoidal estimates in Equation 14 with $b = 20$ to estimate e_0 in French females, 1816–2015**

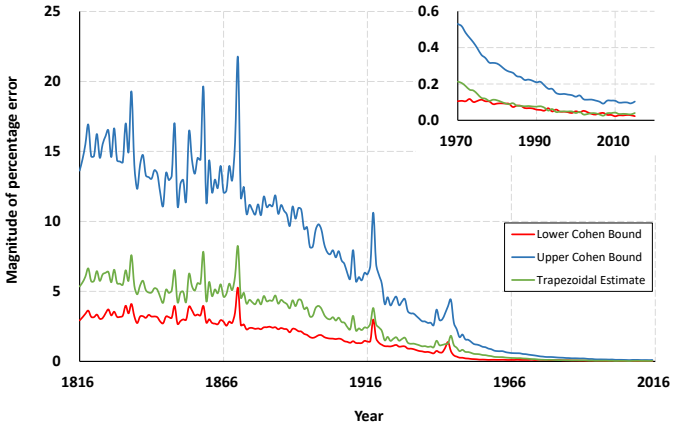

Note: Life table data obtained from the Human Mortality Database (HMD).

Figure 3: **Comparisons of the percentage error in using the lower bounds (red), upper bounds (blue), and trapezoidal estimates in Equation 14 with $b = 40$ to estimate e_0 in French females, 1816–2015**

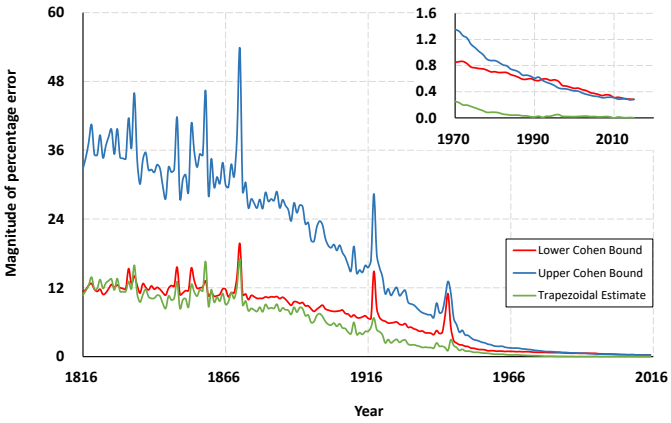

Note: Life table data obtained from the Human Mortality Database (HMD).

Figure 4: Comparisons of the percentage error in using the lower bounds (red), upper bounds (blue), and trapezoidal estimates in Equation 14 with $b = 60$ to estimate e_0 in French females, 1816–2015

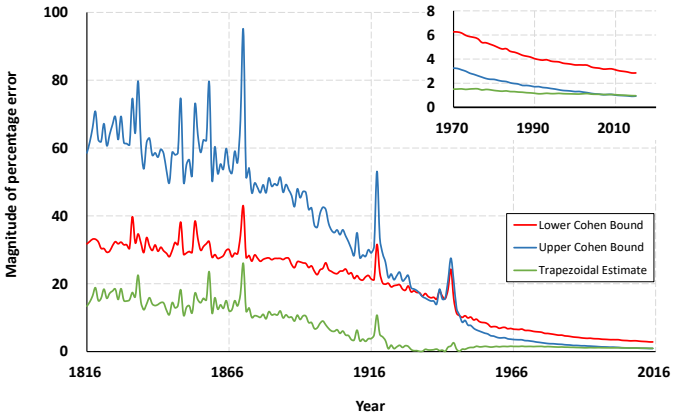

Note: Life table data obtained from the Human Mortality Database (HMD).

Figure 5: Comparisons of the percentage error in using the lower bounds (red), upper bounds (blue), and trapezoidal estimates in Equation 14 with $b = 80$ to estimate e_0 in French females, 1816–2015

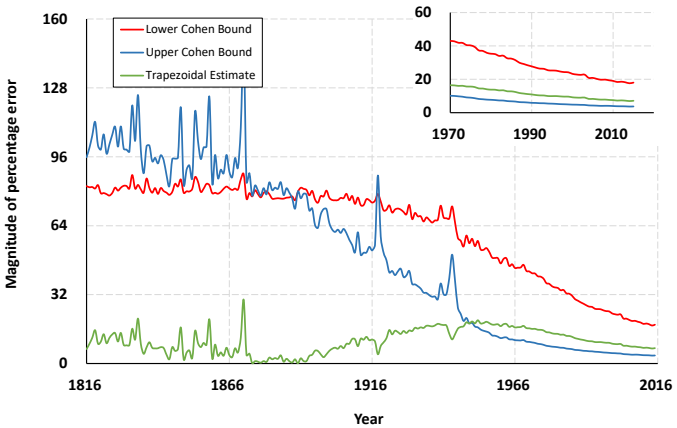

Note: Life table data obtained from the Human Mortality Database (HMD).

Figure 6: Survival curves for French females in 1816 (red), 1866 (blue), 1916 (gold), 1966 (green), and 2015 (black)

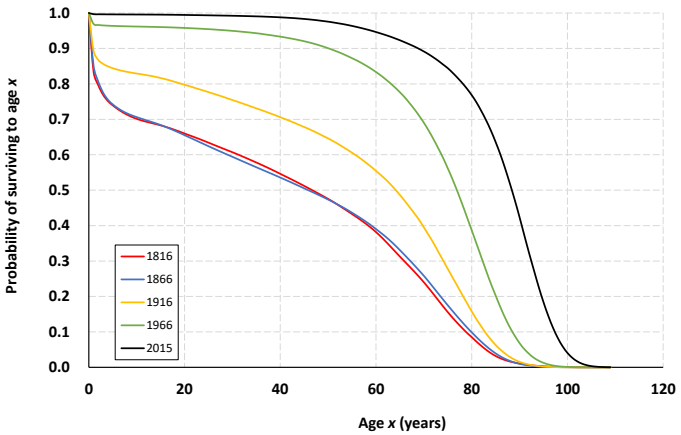

Note: Life table data obtained from the Human Mortality Database (HMD).

We now illustrate Corollary 1. We do not know a priori the corresponding $\xi_{a,b}$-value that will yield the exact $e(a)$-value promised by Equation 9. But a posteriori, once the relevant life table parameters are known (specifically, $e(a)$, $e(b)$, $s(a)$, and $s(b)$), then solving Equation 9 for $\xi_{a,b}$ yields

$$\xi_{a,b} = \frac{1}{s(b) - s(a)} \left[\frac{e(a)s(a) - e(b)s(b)}{b - a} - s(a) \right]. \tag{23}$$

These ξ-values will be closer to 0 than 1 if $s(x)$ is concave on $[a, b]$ and closer to 1 than 0 if $s(x)$ is convex on $[a, b]$. Thus, calculating the ξ-values for consecutive life tables allows us to track the historical trends in those ξ-values in real-world data sets and provides information about how the associated survival curves have evolved over time. Figure 7 illustrates this by comparing the values of $\xi_{0,b}$ for the b-values considered in Figures 2–5. (To be clear, these particular ξ-values yield exact e_0-values.)

Figure 7: **A plot of the $\xi_{0,b}$ values from Equation 23 that yield exact e_0-values for $b = 20$ (blue), 40 (red), 60 (green), and 80 (black) for French females, 1816–2015**

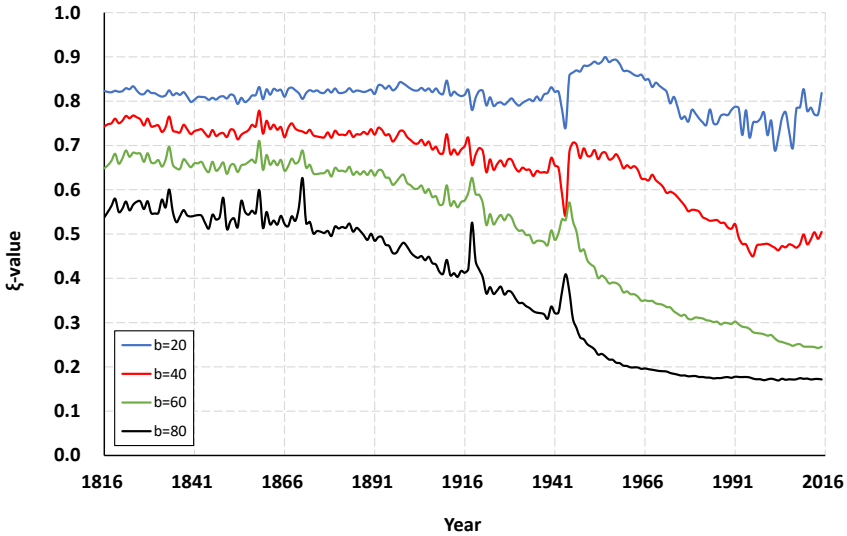

Note: Life table data obtained from the Human Mortality Database (HMD).

We observe that the maximum ξ-values decrease as b increases. This accords with the increasingly concave nature of the survival curves (Figure 6) as both b and time increase. This same concavification of the survival curves over time results in a decreasing trend in $\xi_{0,b}$-values for a fixed b-value. This is particularly prominent in the $b = 80$ (black) curve. As Figure 6 shows, over time the survival curves have become more strongly concave on the interval $0 \leq x \leq 80$, driving down the values of $\xi_{0,80}$. Of the four b-values considered, the $\xi_{0,20}$-values have shown the least variability over time. This suggests that perhaps there is a single ξ-value that can accurately estimate e_0 for the full data set in the $b = 20$ case. Let us denote this single ξ-value by $\xi^*_{0,20}$. To find this ξ^*-value we minimized the root mean square error between e_0 and the estimate in Equation 8 (with $a = 0$ and $b = 20$). This yields $\xi^*_{0,20} \approx 0.8182$ and the corresponding estimates

$$\begin{aligned} e_0 &\approx 20[1 + \xi^*_{0,20}(s(20) - 1)] + e(20)s(20) \\ &= 20\left(1 - \xi^*_{0,20}\right) + s(20)\left(e(20) + 20\xi^*_{0,20}\right) \\ &\approx 3.6359 + s(20)\left(16.3641 + e(20)\right). \end{aligned} \tag{24}$$

Figure 8 plots the percentage error in estimating e_0 with Equation 24. Remarkably, as Figure 8 shows, this approximation yields highly accurate estimates of e_0 (error magnitude less than 0.5%) regardless of the complex and dynamic changes in mortality across age and time in the population since 1816.

Figure 8: **A plot of the percentage errors in approximating e_0 for French females, 1816–2015, using $\xi_{0,20} \approx 0.8182$**

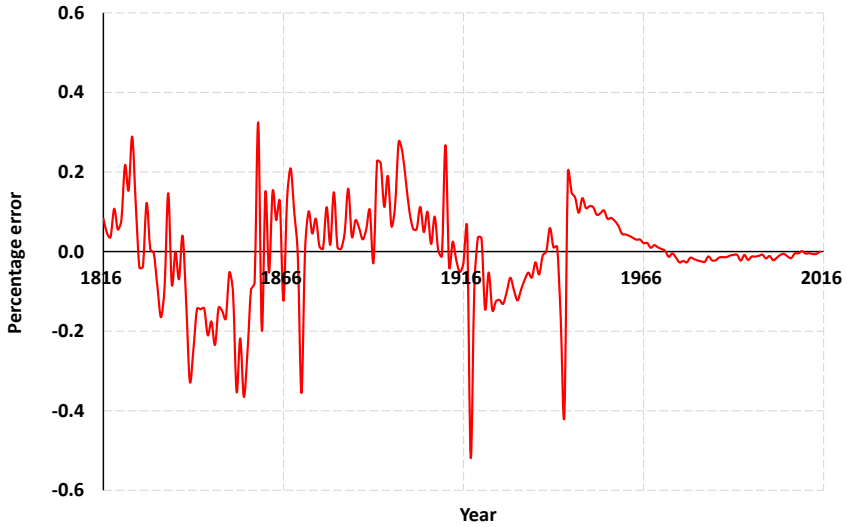

Note: Life table data obtained from the Human Mortality Database (HMD).

5. Discussion

The useful inequalities derived by Cohen (2011) for bounding the remaining life expectancy $e(a)$ emerge from using 0-degree accurate quadrature rules to bound the area under the survival curve, as demonstrated by Equations 3 and 4. By extending this geometric approach, Theorem 2 and Corollary 1 provide conditions under which two-node closed quadrature rules yield 'Cohen inequalities,' and Theorem 3 shows that these yield improvements in the maximum error associated with the Cohen bounds and estimates of $e(a)$, in some cases furnishing exact $e(a)$-values (Equation 9). Section 3.2 showed how these results can be improved via the use of higher-accuracy quadrature rules and/or leveraging information about the concavity of the survival curve. We illustrated our results empirically in Section 4 by studying the French female population post-1816. As we

saw, the concavification of the survival curves over time (Figure 6) drove and predicted the accuracy of the various estimates for e_0 (Figures 2–5). These changes in concavity also drove down, in general, the ξ-values yielding exact e_0-values (Figure 7). The notable exceptions were the $\xi_{0,20}$-values. These varied little enough over time that it became possible to extract highly accurate e_0 estimates for the entire data set (Equation 24 and Figure 8) using only information about $s(20)$ and $e(20)$.

Possible future research could focus particularly on this last point. The highly accurate e_0 estimates in Equation 24 constitute a new regularity in the French female population. At present, this is an empirical regularity attributable to Corollary 1 and the observations regarding the concavity of $s(x)$ made following Equation 23. But one may wonder what, if any, biodemographic drivers may be responsible for this regularity. Why can life expectancy at birth for French females be so accurately estimated over the 200 years between 1816 and 2015 by knowing only $s(20)$ and $e(20)$? Do regularities like Equation 24 extend to other human populations (e.g., other populations in the HMD)? That is, can life expectancy at birth in country i, denoted $e_{0;i}$, be estimated to the same high degree of accuracy by relations of the form

$$e_{0;i} = c_{1;i} + s(b)(c_{2;i} + e(b)), \qquad c_{1;i} = 1 - \xi^*_{0,b;i}, \quad c_{2,i} = b\xi^*_{0,b;i} \tag{25}$$

for some optimal ξ-values $\xi_{0,b;i}$? This is likely the case for at least some other countries in the HMD since the French female population's mortality trajectories are not substantially different from those of other industrialized countries in Europe. What can explain the particular ξ- and b-values yielding the highest accuracy approximations? Perhaps, even in the case of Equation 24, there exists an optimal b-value, perhaps $b \neq 20$, that increases the accuracy of Equation 24 even further. Perhaps there are subsets of HMD countries with similar optimal estimates in Equation 25 including similar b-values. If there are, then in these countries, as for French females since 1816, life expectancy at birth would appear to be intimately tied to the survival probability and remaining life expectancy at a particular age b or over a particular narrow range of b-values. Why would survivorship and remaining life expectancy at such ages be so intimately linked with e_0 in those countries?

The same theory, analyses, and future research questions described above can also be investigated for nonhuman species. Does Equation 25 produce high-accuracy e_0 estimates for nonhuman species? If so, why? If not, what makes humans special? Given that life tables for many nonhuman populations are stage-based and not age-based, answers to these questions could provide useful and practical estimates of life expectancy at birth and perhaps also reveal the existence of hidden ecological, evolutionary, and biodemographic regularities linking life expectancy at birth to later-stage survivorship and remaining life expectancy.

6. Acknowledgments

I thank the John Simon Guggenheim Memorial Foundation for their generous support of this work via the 2021 Guggenheim Fellowship I received. I am also grateful to the reviewers for their many helpful comments and suggestions.

References

Human Mortality Database. University of California, Berkeley (USA), and Max Planck Institute for Demographic Research (Germany). Available at www.mortality.org. Accessed August 2021.

Burden, R., Faires, J., and Burden, A. (2015). *Numerical Analysis.* 10th Ed. Pacific Grove, CA: Brooks/Cole Pub. Co.

Cohen, J. (2011). Life expectancy: Lower and upper bounds from surviving fractions and remaining life expectancy. *Demographic Research* 24(11): 251–256. doi:10.4054.DemRes.123456789.

Stoer, J. and Burlisch, R. (1993). *Introduction to Numerical Analysis.* 2nd Ed. New York, NY: Springer-Verlag.

Weon, B. and Je, J. (2012). Trends in scale and shape of survival curves. *Scientific Reports* 2(504): 1–7. doi:10.1038.srep00504.

Appendix

An approximation of the form

$$\int_a^b s(t)\,dt \approx c_1 s(a) + c_2 s(b) \tag{26}$$

is called a two-node closed (interpolating) quadrature rule in numerical analysis (Burden, Faires, and Burden 2015). Here the c_i are referred to as the weights, the x-values of $s(x)$ used on the right-hand side of Equation 26 are called the nodes, and 'closed' refers to the fact that the nodes include the endpoints of the interval of integration.

The degree of accuracy of a quadrature rule is the largest positive integer n such that the rule is exact for x^k, for each $k = 0, 1, \ldots, n$ (Burden, Faires, and Burden 2015). The simplest two-node closed quadratures (26) are the left- and right-hand Riemann sums, which correspond to $c_1 = (b - a)$ and $c_2 = 0$, and $c_1 = 0$ and $c_2 = (b - a)$, respectively. These are 0-degree accurate quadrature rules: Equation 26 is exact for the aforementioned c-value combinations only when $s(x)$ is constant (x^0) on $[a, b]$.